J Mater Sci (2010) 45:2051–2056
DOI 10.1007/s10853-009-4120-5

HTC2009

Experimental study of density, surface tension, and contact angle of Sn–Sb-based alloys for high temperature soldering

Yu. Plevachuk · W. Hoyer · I. Kaban · M. Köhler · R. Novakovic

Received: 2 June 2009 / Accepted: 9 December 2009 / Published online: 29 December 2009
© Springer Science+Business Media, LLC 2009

Abstract The density and the surface tension of binary Sn–Sb and ternary Sn–Sb–Cu liquid alloys have been measured over a wide temperature range by the sessile-drop method. The experimental data for the surface tension were analyzed by the Butler thermodynamic model. Investigations of the wetting behavior of these alloys on the Cu and Ni substrates in a vacuum were also performed.

Introduction

High-temperature solders with melting temperatures above 500 K are widely used in the electronics industry for advanced packing technologies [1]. In the multi-chip modeling (MCM) technology, there is a need for a family of solder alloys with different melting temperature (the upper limit is around 620 K). Availability of different solders enables complex electronic components to be manufactured. The Sn-based alloys with antimony are possible substitutes for the toxic high-temperature Pb–Sn solders (>85 wt% Pb) currently used in the MCM technology, due to the improvement of wetting properties, thermal fatigue resistance, and creep strength [2]. Sn–Sb solders with good electrical properties and different melting points are often used in the step soldering technology, where soldering is applied more than once during the manufacturing. The solders used at the early stages should be characterized by higher melting temperatures in order to prevent melting of the existing solder joints during the subsequent soldering [3].

Small quantities of copper are often added to the solder alloys for improvement of their electrical characteristics, changing the melting temperature, and to prevent the whisker formation. Cu is also introduced into the solder due to the dissolution of Cu substrate. Therefore, it is important to know the effect of Cu on the solderability, when selecting a particular Sn–Sb–Cu solder alloy.

Among various physical properties, the knowledge of the surface tension is very important for practical applications because it is directly related to the wettability of a substrate by a solder. If an addition of some component to a liquid alloy decreases the surface tension, the wettability is improved simultaneously. Hence, measurements of the surface tension are useful for predicting the effect of modifying elements on the solder properties. Experimental data on the surface tension, density, and wetting behavior are scarce in the literature and rather contradictory even for binary Sn–Sb alloys. Also, their properties are not well known, particularly with respect to their interactions with substrate materials [4–7]. In the present work the thermophysical properties relevant to the soldering process, namely, density, surface tension, and the wetting behavior on the Cu and Ni substrates for some binary Sn–Sb and ternary Sn–Sb–Cu liquid alloys have been investigated over a wide temperature range by the sessile-drop method.

Yu. Plevachuk (✉)
Department of Metal Physics, Ivan Franko National University, 79005 Lviv, Ukraine
e-mail: plevachuk@mail.lviv.ua

W. Hoyer · I. Kaban
Institute of Physics, Chemnitz University of Technology, 09107 Chemnitz, Germany

M. Köhler
German Aerospace Center, Institute of Materials Physics in Space, 51170 Cologne, Germany

R. Novakovic
Department of Genoa, CNR-IENI, Via de Marini, 6, 16149 Genoa, Italy

Experimental details

In this work, the density, surface tension, and wetting behavior were studied by means of the sessile-drop technique, where the profile of a liquid droplet placed on a substrate is recorded and analyzed. The basic method is well established and described in various textbooks, for example [8].

The alloys have been prepared from pure Sn, Sb, and Cu (99.99%) according to the nominal composition by arc melting under protective atmosphere of high purity argon after preliminary evacuation of the furnace up to the rest pressure $\approx$0.1 Pa. Almost spherical specimens of about 15–25 mm^3 were placed on polished graphite substrates for the density and surface tension measurements. Before the measurements the graphite substrates were aligned horizontally in order to provide an axis-symmetry of the liquid drop. The axis-symmetry of the sample was checked permanently during the experimental run. The shape of the sample was captured by means of a digital CCD camera at a rate of 25 frames/s. Three series comprising 20 pictures each were captured during 2 min after reaching the desired temperature.

The temperature was measured with a thermocouple (type K) placed right above the sample and kept stable within $\pm$1 K around the selected set point. During the experiments a pressure of less than 10^{-3} Pa was maintained in the chamber. Measurements of the density and surface tension were started at the maximum experimental temperature. Images were taken at intervals of about 25 K after a slow cooling and temperature stabilization for several minutes. In order to avoid recording of the glowing of the heater and samples, monochromatic blue background light and a suitable filter in front of the camera were applied.

In order to obtain the density and the surface tension the droplet shape was analyzed. The substrate line and the profile of the sample were found automatically by dedicated evaluation software [9]. Assuming cylindrical symmetry, a contour function has been obtained and then integrated in order to get the volume and, finally, with the sample mass, the density, ρ.

Determination of the surface tension, σ, is based on the analysis given by Rotenberg et al. [10]. Starting from suitable assumptions on the droplet size and its surface tension, the profile line was calculated by numerical integration of the Laplace equation. Studying the experimental and analysis procedure one can estimate that the relative experimental uncertainty of the obtained density is less than 7%. The capillary parameter can be determined to an accuracy of about 5%. Consequently, the overall relative error of the surface tension can be estimated to be of about 12% [9].

For investigation of the contact angle, copper and nickel plates were used as substrates. Prior to the measurement, the surface of the substrate was carefully polished, cleaned with acid, and rinsed with propane.

In order to achieve a uniform temperature field, at the beginning of each measurement the alloy sample was kept 15 min in the furnace at the temperature of about 20 K below its melting temperature. The measurements were carried out with steps of temperature between 10 and 20 K.

Modeling

The surface tension of binary and ternary liquid alloys can be calculated with the equation of Butler [11]:

$$\sigma = \sigma_i + \frac{RT}{S_i}\ln\frac{X_i^s}{X_i^b} + \frac{1}{S_i}\left[G_i^{xs,s}\left(T, X^s_{j(j=2,3)}\right) - G_i^{xs,b}\left(T, X^b_{j(j=2,3)}\right)\right], \quad i = 1,2,3. \tag{1}$$

where R, T, σ_i, S_i are gas constant, temperature, surface tension of pure components, and surface area, respectively. $G_i^{xs,s}\left(T, X^s_{j(j=2,3)}\right)$ and $G_i^{xs,b}\left(T, X^b_{j(j=2,3)}\right)$ are partial excess Gibbs's energies of a component i in the surface phase and in the bulk phase, respectively. Both free energies are given as functions of T and composition of the surface and bulk phase, i.e., $X^s_{j(j=2,3)}$ and $X^b_{j(j=2,3)}$.

The surface area of component i is calculated from the Avogadro's number, the atomic mass, and the density data [8] as follows:

$$S_i = 1.091 N_0 \left(\frac{M_i}{\rho_i}\right)^{2/3} \tag{2}$$

The excess energy term of a component i can be derived from the standard thermodynamic relation, in the form:

$$G_i^{xs} = G^{xs} + \sum_{j=1}^{n} (\delta_{ij} - X_j)\frac{\partial G^{xs}}{\partial X_j} \tag{3}$$

where δ_{ij} is Kronecker's symbol.

Assuming that the free energy of the alloy is always proportional to the number interactive contacts between neighboring atoms, $G_i^{xs,b}$ and $G_i^{xs,s}$ can be related to the respective coordination numbers in the surface layer and the bulk phase as:

$$G_i^{xs,s}\left(T, X^s_{j(j=2,3)}\right) = \beta G_i^{xs,b}\left(T, X^b_{j(j=2,3)}\right) \tag{4}$$

where β is the ratio between the two coordination numbers, i.e., a parameter describing the reduced coordination in the liquid phase. In typical close-packed solid structures (bcc, hcp) the coordination numbers are 12 and 9 for the bulk and the surface phases, respectively, and thus $\beta = 0.75$.

However, in some cases the value of β might be affected by other factors, such as the relaxation of the surface structure, and in the literature different values ranged in $0.5 \leq \beta \leq 0.84$ can be found [12].

Results and discussion

The density, surface tension, and contact angle measurements were performed for binary Sn–Sb and ternary Sn–Sb–Cu liquid alloys between their melting point, T_m, and 873 K. The temperature dependence of the surface tension, $\sigma(T)$, of molten binary $Sn_{90}Sb_{10}$, $Sn_{80}Sb_{20}$ and ternary $Sn_{90.8}Sb_{7.4}Cu_{1.8}$, $Sn_{83.84}Sb_{12.99}Cu_{3.17}$, $Sn_{76.1}Sb_{20.2}Cu_{3.7}$ liquid alloys (all in at.%) is shown in Fig. 1 together with the results of previous studies for the alloy compositions close to ours [4]. The surface tension decreases linearly with increasing temperature and can be presented as:

$$\sigma = \sigma_0 + \frac{d\sigma}{dT}(T - T_m) \quad (5)$$

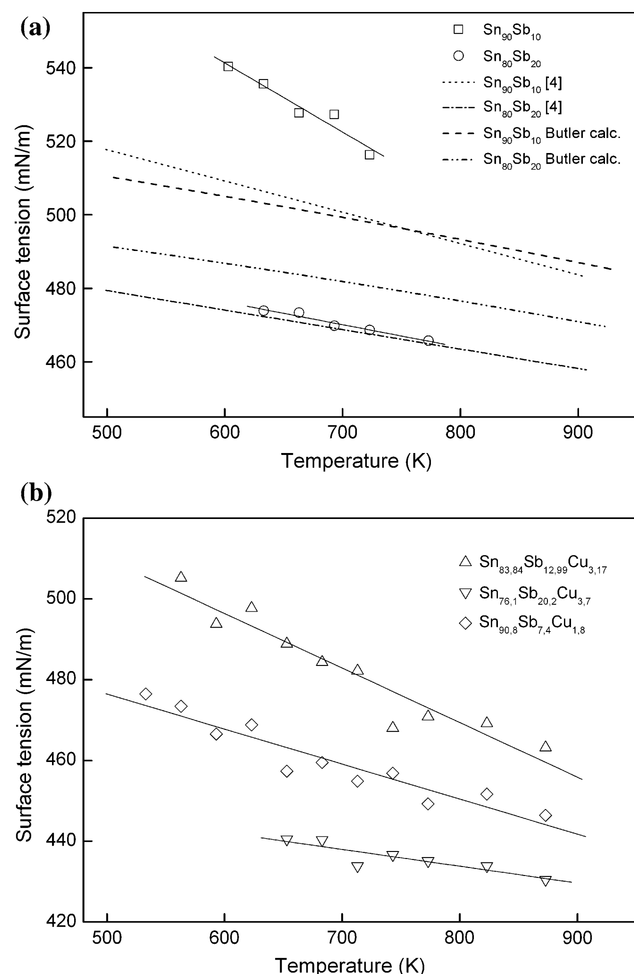

Fig. 1 Temperature dependence of the surface tension for the Sn–Sb (**a**) and Sn–Sb–Cu (**b**) liquid alloys

Table 1 Temperature dependence of the surface tension of the Sn–Sb and Sn–Sb–Cu liquid alloys

Alloy	σ_0, mN/m	$d\sigma/dT$, mN/m/K	T_m, K
$Sn_{90}Sb_{10}$	555	−0.19	544
$Sn_{80}Sb_{20}$	476	−0.06	593
$Sn_{90.8}Sb_{7.4}Cu_{1.8}$	475	−0.09	513
$Sn_{83.84}Sb_{12.99}Cu_{3.17}$	503	−0.13	548
$Sn_{76.1}Sb_{20.2}Cu_{3.7}$	445	−0.07	592

where σ_0 is the surface tension at the melting temperature T_m, and $d\sigma/dT$ is the surface tension temperature coefficient.

For each of the samples investigated the data obtained by our measurements can be described by Eq. 5 with parameters σ_0 and $d\sigma/dT$ listed in Table 1. The magnitude of the surface tension increases with an increase of the Sn-content for the binary $Sn_{90}Sb_{10}$ and $Sn_{80}Sb_{20}$ alloy. The surface tension of the molten $Sn_{90}Sb_{10}$ is higher than the corresponding value obtained by the maximum bubble pressure method [4], while the data of the $Sn_{80}Sb_{20}$ alloy are in good agreement.

It should be noted that among all methods, the sessile-drop method and the maximum bubble pressure method are most easily applied at elevated temperatures and have been most frequently used [13]. Although the maximum bubble pressure technique frequently produces lower values [14], the present results agree with data reported in [4] as well as with the theoretical values calculated by the Butler's model in the regular solution approximation within the experimental error.

The situation with the surface tension data of ternary alloys is more complicated. The lowest $\sigma(T)$ corresponds to the composition with the lowest Sn-content, $Sn_{76.1}Sb_{20.2}Cu_{3.7}$. Positions of the other two dependencies reflect the influence of the both elements (antimony and copper) on the surface tension of liquid tin.

The values of the Gibbs free energy of mixing, G_M of liquid Sn–Sb phase determined experimentally [15] and obtained from the thermodynamic calculations [16] are very similar for the equiatomic composition (in the normalized form, G_M/RT equals –0.9270 and –0.9345 at 873 K, respectively), which indicates weak interatomic interactions in the alloy melts. The surface tension isotherm of liquid Sn–Sb alloys calculated by the Butler's model in the regular solution approximation at 873 K together with that obtained in the ideal solution approximation is shown in Fig. 2. The regular solution isotherm deviates positively from the corresponding ideal solution curve, confirming that liquid alloys with negative excess Gibbs energy in the bulk exhibit positive surface tension deviations with respect to the ideal mixture. The surface tension literature data [4] of Sb- and Sn-rich alloys exhibit

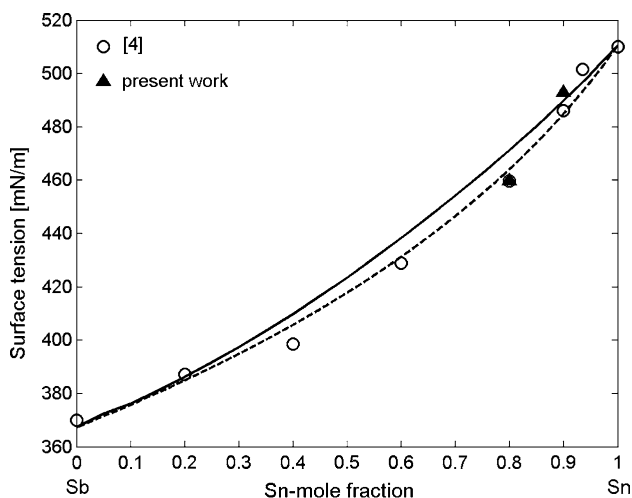

Fig. 2 Surface tension of liquid Sn–Sb alloys calculated at T = 873 K. *Open circle* refers to the literature data, [4] and *filled triangle* are the experimental data of present work. (*solid line* Butler model in the regular solution approximation; *dashed line* the ideal solution model)

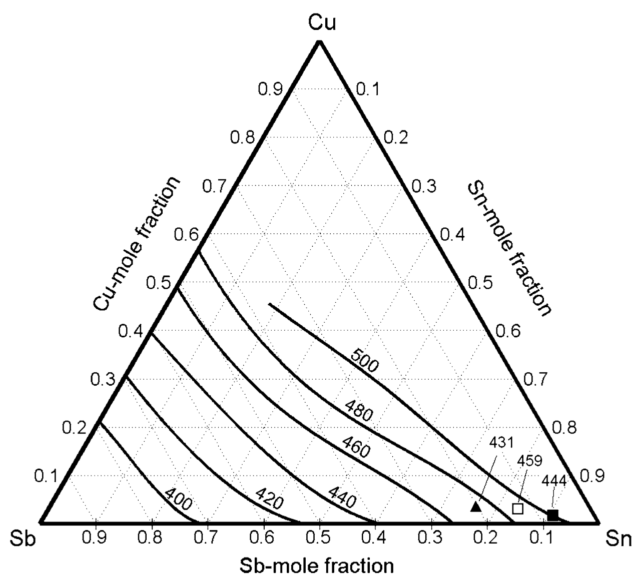

Fig. 3 Iso-surface tension lines (in mN/m) of liquid Sn–Sb–Cu alloys calculated by the Butler model in the regular solution approximation at 873 K. The symbols represent the alloys studied: $Sn_{90.8}Sb_{7.4}Cu_{1.8}$ (*filled square*), $Sn_{83.84}Sb_{12.99}Cu_{3.17}$ (*open square*), $Sn_{76.1}Sb_{20.2}Cu_{3.7}$ (*filled triangle*). The experimental values of the surface tension are also given

a good agreement with the calculated values obtained by the Butler's model in the regular solution approximation, while differ slightly from the corresponding data of Sn–Sb alloys having intermediate compositions. The same trend is noted for our surface tension experimental data of $Sn_{90}Sb_{10}$ and $Sn_{80}Sb_{20}$ alloys (Fig. 2).

The surface tension of liquid Sn–Sb–Cu alloys was calculated with by Eq. 1 along with Eqs. 2–4 using the Gibbs free energy data of the liquid binary phases Sb–Sn [15], Cu–Sn [17], and Cu–Sb [18], while the surface tension of pure components and structural data (coordination number, molar volume) were taken from [8]. The difference between the surface tension of liquid $Sn_{90.8}Sb_{7.4}Cu_{1.8}$, $Sn_{83.84}Sb_{12.99}Cu_{3.17}$, and $Sn_{76.1}Sb_{20.2}Cu_{3.7}$ at 873 K obtained experimentally and the values calculated with the Butler's model in the regular solution approximation is up to about 8% (Fig. 3).

The density values of molten binary $Sn_{90}Sb_{10}$, $Sn_{80}Sb_{20}$ and ternary $Sn_{90.8}Sb_{7.4}Cu_{1.8}$, $Sn_{83.84}Sb_{12.99}Cu_{3.17}$, $Sn_{76.1}Sb_{20.2}Cu_{3.7}$ liquid alloys are shown in Fig. 4. The temperature dependence of the density in the temperature interval investigated can be well fitted with linear functions for all compositions:

$$\rho = \rho_0 + \frac{d\rho}{dT}(T - T_m) \quad (6)$$

where ρ_0 is the density at the melting temperature, and $d\rho/dT$ is the thermal coefficient of the density. The parameters ρ_0 and $d\rho/dT$ obtained by fitting of the experimental data are listed in Table 2. The obtained values of the density of liquid Sb–Sn alloys are in good agreement with the data reported earlier in [5].

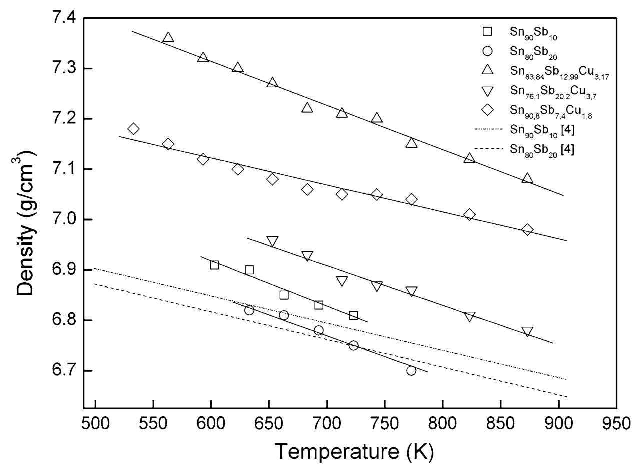

Fig. 4 Temperature dependence of the density for the Sn–Sb and Sn–Sb–Cu liquid alloys

Table 2 The temperature dependence of the density for the studied liquid alloys: linear fits of the experimental data plotted in Fig. 4

Alloy	ρ_0, g/cm^3	$d\rho/dT$, 10^{-4} g/cm^3/K	T_m, K
$Sn_{90}Sb_{10}$	6.97	−9.00	544
$Sn_{80}Sb_{20}$	6.86	−8.27	593
$Sn_{90.8}Sb_{7.4}Cu_{1.8}$	7.17	−5.35	513
$Sn_{83.84}Sb_{12.99}Cu_{3.17}$	7.36	−8.76	548
$Sn_{76.1}Sb_{20.2}Cu_{3.7}$	6.99	−7.90	592

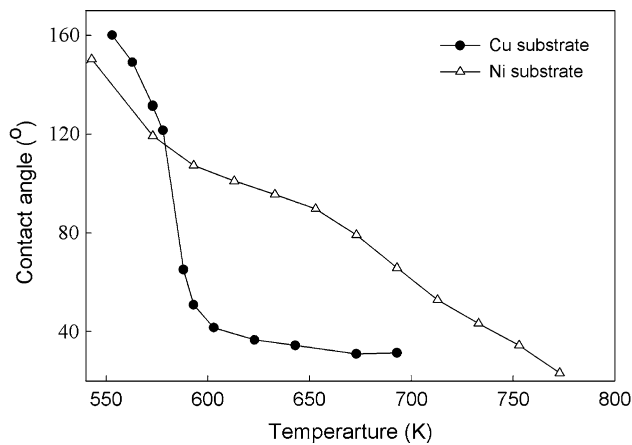

Fig. 5 Temperature dependence of the contact angle of the liquid $Sn_{90.8}Sb_{7.4}Cu_{1.8}$ alloy on copper and nickel substrates

The contact angles of molten binary $Sn_{95}Sb_5$, $Sn_{90}Sb_{10}$, $Sn_{80}Sb_{20}$ and ternary $Sn_{90.8}Sb_{7.4}Cu_{1.8}$, $Sn_{83.84}Sb_{12.99}Cu_{3.17}$, $Sn_{76.1}Sb_{20.2}Cu_{3.7}$ liquid alloys were determined. Temperature dependence of the contact angle, θ, for the $Sn_{90.8}Sb_{7.4}Cu_{1.8}$ liquid alloy on the copper and nickel substrates is presented in Fig. 5. As can be seen, the contact angle slightly decreases at low temperature. Then, a rapid decrease from 120° to about 40° in a narrow temperature range between 573 and 593 K takes place. Further heating up to about 673 K is accompanied by a gradual contact angle decreasing to its lowest value of 31°. Similar wetting behavior on the copper substrate was observed for other alloys, while temperature behavior of their contact angle on the nickel substrate differs noticeably. The contact angle on the nickel substrate of the $Sn_{90.8}Sb_{7.4}Cu_{1.8}$ liquid alloy decreases gradually with heating from initial 150° to the lowest value of about 20°. Such a gradual $\theta(T)$ decreasing has been revealed both in the binary and ternary alloys. The present results are in agreement with [19–21], confirming different wetting behavior of Sn-based solders in contact with copper and nickel substrates. Namely, a sharp drop of the contact angle after only few seconds was already observed dealing with Sn-rich solder alloys and Cu substrate, while a stepwise decrease of the contact angle is characteristic for the same type of alloys in contact with Ni substrate [19–21]. These results are related to the higher rate of dissolution controlled by diffusion in the liquid phase in the case of copper substrate. It was found that Cu atoms diffuse faster into the solder comparing to those of Ni [22, 23] and the intermetallic compounds of different thickness are formed at the interface [19]. An influence of the thickest Cu_5Sn_6 layer could be the reason of a sharp decrease of the contact angle on the Cu substrate, connected with reaching the so-called temperature threshold of wetting (see [24] and references therein].

Table 3 Contact angles and temperature values for the liquid alloy/substrate systems studied

Alloy	Cu substrate			Ni substrate		
	θ°	T, K	T (θ = 40°), K	θ°	T, K	T (θ = 40°), K
$Sn_{95}Sb_5$	28	683	668			
$Sn_{90}Sb_{10}$	26	663	643			
$Sn_{80}Sb_{20}$	43	684				
$Sn_{90.8}Sb_{7.4}Cu_{1.8}$	31	673	593	20	773	740
$Sn_{83.84}Sb_{12.99}Cu_{3.17}$	45	723		38	713	710
$Sn_{76.1}Sb_{20.2}Cu_{3.7}$	26	673	618	42	723	

The minimum contact angle values for the alloys and substrates investigated as well as the corresponding initial temperatures are summarized in Table 3. Taking into account that for the solder alloys, the contact angle of 40° indicates a good wettability, the corresponding temperatures are also reported.

It is evident that the wetting of copper by liquid Sn–Sb alloys is better in comparison with the wetting of nickel. Upon addition of copper, the wetting of nickel substrates by Sn–Sb–Cu alloy melts becomes worse. The contact angles of ternary compositions measured on the copper substrate strongly depend on the Sn/Sb/Cu ratio in the alloy (Table 3).

Summary

The density, surface tension, and wetting on the Cu and Ni substrates have been studied for liquid Sn–Sb and Sn–Sb–Cu alloys in the temperature range from their melting point up to 873 K. Corresponding linear dependences have been derived for the surface tension and density. The results obtained, compared to available literature data exhibit a good agreement. The surface tension data have also been analyzed by the thermodynamic model based on the Butler equation. The experimental surface tension, density, and contact angle data provide useful information for development of new materials for high-temperature soldering.

Acknowledgements This work was performed in the framework of the European Concerted Research Action COST MP0602 project: "Advanced Solder Materials for High Temperature Application". The authors acknowledge the financial support of this work by the Deutscher Akademischer Austausch Dienst - German Academic Exchange Service (DAAD).

References

1. Gayle F, Becka G, Badgett J, Whitten G, Pan T, Grusd A, Bauer B, Lathrop R, Slattery J, Anderson I, Foley J, Gickler A, Napp D, Mather J, Olson C (2001) JOM 53(6):17

2. Lee HT, Chen MH, Jao HM, Hsu CJ (2004) J Electron Mater 33:1048
3. Chen S, Chen P, Wang C (2006) J Electron Mater 35:1982
4. Gasior W, Moser Z, Pstrus J (2003) J Phase Equilib 24(6):504
5. Lee BJ, Lee HM (1997) In: Mahidhara RK et al (eds) Design and reliability of solder and solder interconnections. TMS, Warrendale, PA, p 129
6. Jang JW, Kim PG, Tu KN (1999) J Mater Res 14:3895
7. Kim JH, Jeong SW, Lee HM (2002) Mater Trans 43:1873
8. Iida T, Guthrie RIL (1993) The physical properties of liquid metals. Clarendon Press, Oxford
9. Gruner S, Köhler M, Hoyer W (2009) J Alloys Compd 482:335
10. Rotenberg Y, Boruvka L, Neumann AW (1983) J Colloid Interface Sci 93:169
11. Butler JAV (1932) Proc Roy Soc A135:348
12. Tanaka T, Hack K, Hara S (1999) MRS Bull 24:45
13. Keene BJ (1993) Int Mater Rev 38(4):157
14. Gasior W, Moser Z, Pstrus J (2001) J Phase Equilib 22:20
15. Hultgren R, Desai PD, Hawkins DT, Gleiser M, Kelly KK (1973) Selected values of thermodynamics properties of binary alloys. ASM International, Metals Park, OH, pp 1300–1305
16. Jönsson B, Ågren J (1986) Mater Sci Technol 2:913
17. Miettinen J (2004) Calphad 28:71
18. Liu XJ, Wang CP, Ohnuma I, Kainuma R, Ishida K (2000) J Phase Equilib 21:432
19. Rizvi MJ, Chan YC, Bailey C, Lu H, Islam MN, Wu BY (2005) J Electron Mater 34:1115
20. Gnecco F, Ricci E, Amore S, Giuranno D, Borzone G, Zanicchi G, Novakovic R (2007) Int J Adhes Adhes 27(5):409
21. Amore S, Ricci E, Borzone G, Novakovic R (2008) Mater Sci Eng A Struct Mater A495(1–2):108
22. Ghosh G (2001) Acta Mater 49:2609
23. Rizvi MJ, Lu H, Bailey C (2009) Thin Solid Films 517:1686
24. Gubzhokov MM, Ponegev MKh, Sozaeva AB, Sozaev VA (2008) J Phys Conf Series 98:062028